The EMBO Journal (2012) 31, 4428–4440 | © 2012 European Molecular Biology Organization | All Rights Reserved 0261-4189/12
www.embojournal.org

THE EMBO JOURNAL

Reciprocal expression of MRTF-A and myocardin is crucial for pathological vascular remodelling in mice

Takeya Minami[1], Koichiro Kuwahara[1,*], Yasuaki Nakagawa[1], Minoru Takaoka[2], Hideyuki Kinoshita[1], Kazuhiro Nakao[1], Yoshihiro Kuwabara[1], Yuko Yamada[1], Chinatsu Yamada[1], Junko Shibata[1], Satoru Usami[1], Shinji Yasuno[3], Toshio Nishikimi[1], Kenji Ueshima[3], Masataka Sata[4], Hiroyasu Nakano[5], Takahiro Seno[6], Yutaka Kawahito[6], Kenji Sobue[7], Akinori Kimura[8], Ryozo Nagai[2] and Kazuwa Nakao[1]

[1]Department of Medicine and Clinical Science, Kyoto University Graduate School of Medicine, Kyoto, Japan, [2]Department of Cardiovascular Medicine, Graduate School of Medicine, The University of Tokyo, Tokyo, Japan, [3]EBM Research Center, Kyoto University Graduate School of Medicine, Kyoto, Japan, [4]Department of Cardiovascular Medicine, Institute of Health Biosciences, The University of Tokushima Graduate School, Tokushima, Japan, [5]Laboratory of Molecular and Biochemical Research, Department of Immunology, Biomedical Research Center, Juntendo University Graduate School of Medicine, Tokyo, Japan, [6]Department of Inflammation and Immunology, Graduate School of Medical Science, Kyoto Prefectural University of Medicine, Kyoto, Japan, [7]Department of Neuroscience, Institute for Biomedical Sciences, Iwate Medical University, Iwate, Japan and [8]Department of Molecular Pathogenesis, Medical Research Institute, Tokyo Medical and Dental University, Tokyo, Japan

Myocardin-related transcription factor (MRTF)-A is a Rho signalling-responsive co-activator of serum response factor (SRF). Here, we show that induction of MRTF-A expression is key to pathological vascular remodelling. MRTF-A expression was significantly higher in the wire-injured femoral arteries of wild-type mice and in the atherosclerotic aortic tissues of ApoE$^{-/-}$ mice than in healthy control tissues, whereas myocardin expression was significantly lower. Both neointima formation in wire-injured femoral arteries in MRTF-A knockout (*Mkl1*$^{-/-}$) mice and atherosclerotic lesions in *Mkl1*$^{-/-}$; *ApoE*$^{-/-}$ mice were significantly attenuated. Expression of vinculin, matrix metallopeptidase 9 (MMP-9) and integrin β1, three SRF targets and key regulators of cell migration, in injured arteries was significantly weaker in *Mkl1*$^{-/-}$ mice than in wild-type mice. In cultured vascular smooth muscle cells (VSMCs), knocking down MRTF-A reduced expression of these genes and significantly impaired cell migration. Underlying the increased MRTF-A expression in dedifferentiated VSMCs was the downregulation of microRNA-1. Moreover, the MRTF-A inhibitor CCG1423 significantly reduced neointima formation following wire injury in mice. MRTF-A could thus be a novel therapeutic target for the treatment of vascular diseases.

The EMBO Journal (2012) 31, 4428–4440. doi:10.1038/emboj.2012.296; Published online 26 October 2012
Subject Categories: molecular biology of disease
Keywords: atherosclerosis; muscle, smooth; remodelling; signal transduction

Introduction

It is now recognized that modulation of vascular smooth muscle cell (VSMC) phenotypes plays a key role in the progression of several prominent cardiovascular disease states, including atherosclerosis, hypertension and restenosis (Schwartz *et al*, 1995; Owens *et al*, 2004). Pathological stress induces a switch from a differentiated VSMC phenotype, characterized by strong expression of contractile proteins and little capacity for migration or proliferation, to a proliferative dedifferentiated phenotype, characterized by relatively weak expression of contractile proteins and an increased capacity for migration and proliferation (Watanabe *et al*, 1999; Owens *et al*, 2004; Nishimura *et al*, 2006). VSMC proliferation and migration contribute to vascular remodelling and obstructive vasculopathies such as atherosclerosis and restenosis following percutaneous coronary intervention (Schwartz *et al*, 1995; Bentzon *et al*, 2006). Cytokines and growth factors locally secreted from cells within the vessel and infiltrating inflammatory cells induce migratory and proliferative responses in VSMCs during vascular remodelling (Owens *et al*, 2004), but the intracellular signalling pathways and the transcriptional regulators of phenotypic modulation of VSMCs are incompletely understood.

Myocardin, myocardin-related transcription factor (MRTF)-A (Mkl1, Bsac or Mal) and MRTF-B (Mkl2) are transcriptional cofactors that associate with serum response factor (SRF), an MADS box transcription factor and critical modulator of cardiovascular differentiation and growth, promoting transcription of a subset of genes involved in cytoskeletal organization and muscle differentiation (Wang *et al*, 2001, 2002; Miano, 2003; Olson and Nordheim, 2010). Myocardin, which is highly restricted to smooth and cardiac muscle cell lineages, is located constitutively in the nucleus and strongly activates transcription of SRF-regulated genes, thereby playing an important role in the differentiation and maintenance of cardiac and smooth muscle cell lineage. By contrast, MRTF-A and -B are expressed more ubiquitously and are found in both the cytoplasm and nucleus. In serum-starved fibroblasts, MRTF-A and -B are localized mainly in the cytoplasm and are translocated into the nucleus in response to stimulation with serum or other

*Corresponding author. Department of Medicine and Clinical Science, Kyoto University Graduate School of Medicine, 54 Shogoin Kawaharacho, Sakyo-ku, Kyoto 606-8507, Japan. Tel.: +81 75 751 4287; Fax: +81 75 771 9452; E-mail: kuwa@kuhp.kyoto-u.ac.jp

Received: 13 May 2012; accepted: 2 October 2012; published online: 26 October 2012

stimuli that promote Rho family GTPase activation and subsequent actin polymerization (Kuwahara *et al*, 2005; Nakamura *et al*, 2010; Olson and Nordheim, 2010). Thus, MRTF-A and -B transduce Rho family GTPase-actin signalling from the cytoplasm to SRF in the nucleus (Miralles *et al*, 2003).

Myocardin knockout leads to death *in utero* due to defects in vascular development (Li *et al*, 2003). In addition, myocardin mRNA levels have been shown to be downregulated in dedifferentiated VSMCs during vascular diseases (Liu *et al*, 2005; Chen *et al*, 2011). In contrast to myocardin, the roles played by MRTF-A in VSMC differentiation and phenotypic modulation remain unclear, though a recent human genetic analysis detected an association between coronary artery disease (CAD) and a single-nucleotide polymorphism (SNP) in the promoter region of the MRTF-A gene that enhances the gene expression (Hinohara *et al*, 2009). Li *et al* (2006) reported that MRTF-A knockout mice were born in anticipated Mendelian ratios, whereas Sun *et al* (2006) reported that MRTF-A knockout mice were born at less than the anticipated Mendelian ratio, which they attributed to fetal loss due to heart failure. In both groups, however, live born MRTF-A knockout pups showed no obvious gross abnormality or cardiovascular defect under normal conditions, except for a defect in maternal lactation due to impaired phenotypic modulation of mammary gland myoepithelial cells (Li *et al*, 2006; Sun *et al*, 2006).

In the present study, we investigated the potential roles of MRTF-A in the pathological processes underlying vascular proliferative diseases. We found that induction of MRTF-A expression is key to pathological remodelling underlying vascular disorders, as it sustains the SRF activity necessary for dedifferentiated VSMCs to acquire the capacity to migrate in response to extracellular stimuli. Our findings suggest that the reciprocal expression of MRTF-A and myocardin is mediated, at least in part, by microRNA (miR)-1 and contributes to the phenotypic modulation of VSMCs during vascular remodelling. These results point to MRTF-A as a potentially useful therapeutic target for the treatment of vascular diseases.

Results

Increased expression of MRTF-A in femoral arteries after wire injury

To explore the potential role played by MRTF-A during pathological vascular remodelling, we initially compared the expression of myocardin, MRTF-A and MRTF-B mRNA between femoral arteries subjected to wire injury or to a sham operation. As seen previously (Liu *et al*, 2005; Chen *et al*, 2011), levels of myocardin mRNA were significantly downregulated in femoral arteries 2 weeks after wire injury, while levels of MRTF-B mRNA were not significantly affected (Figure 1A). By contrast, expression of MRTF-A mRNA was significantly increased in injured arteries, as compared to sham-operated arteries (Figure 1A). Western blot analysis using specific antibodies for myocardin, MRTF-A and MRTF-B, respectively, clearly showed that the level of myocardin protein was reduced in injured arteries, whereas MRTF-A protein was significantly increased (Figure 1B and C; Supplementary Figure S1A). Immunohistochemical analysis showed that cells positively stained for MRTF-A were located mainly in the neointima of injured arteries (Figure 1D; Supplementary Figure S1B). Moreover, in serial sections stained for α-smooth muscle actin (αSMA) and smooth muscle myosin heavy chain (SM-MHC), most of the cells that positively stained for MRTF-A also positively stained for both αSMA and SM-MHC (Figure 1D). Time-course analysis of MRTF-A and myocardin expression revealed that MRTF-A mRNA levels were significantly increased by 2 weeks after injury, when dedifferentiated neointimal VSMCs expressing a relatively low level of αSMA were increasing (Shoji *et al*, 2004; Daniel *et al*, 2010). By 50 days after injury, when a more differentiated population of VSMCs is restored (Daniel *et al*, 2010), MRTF-A mRNA had declined to levels comparable to those seen on day 0 (Supplementary Figure S1C). By contrast, myocardin mRNA levels declined continuously for 2 weeks after injury, but had recovered by 50 days after injury (Supplementary Figure S1D). These results suggest that MRTF-A expression is upregulated in activated, dedifferentiated VSMCs during vascular remodelling, while myocardin expression is downregulated in these cells.

Attenuated vascular remodelling after wire injury in MRTF-A knockout mice

To further evaluate the function of MRTF-A during vascular remodelling, next we performed wire injury in the femoral arteries of MRTF-A knockout (*Mkl1*$^{-/-}$) mice. As previously reported, the *Mkl1*$^{-/-}$ mice were viable, fertile and showed no significant gross abnormalities or cardiovascular defects under normal conditions (Li *et al*, 2006). There was no difference in blood pressure or heart rate between wild-type and *Mkl1*$^{-/-}$ mice (Figure 2A), and the thickness of the medial wall in the uninjured sham-operated femoral arteries was comparable between wild-type and *Mkl1*$^{-/-}$ mice (Table I). Femoral arterial expression of myocardin mRNA was significantly weaker in *Mkl1*$^{-/-}$ mice 2 weeks after wire injury than in sham-operated arteries, just as was observed with wild-type mice (Figure 2B). On the other hand, neointima-to-medial ratios determined 4 weeks after wire injury were significantly smaller in *Mkl1*$^{-/-}$ mice than in wild-type mice, whereas there was no difference in medial thickness in the injured arteries between wild-type and *Mkl1*$^{-/-}$ mice (Figure 2C and D; Table I).

Four weeks after wire injury, the neointimal area comprised cells positively stained for αSMA was markedly smaller in *Mkl1*$^{-/-}$ mice than in wild-type mice (Figure 2D). Immunohistochemical analysis in serial sections stained for SM-MHC showed overlap with αSMA-positive cells (Figure 2D), suggesting that a reduction in the numbers of dedifferentiated VSMCs within the neointima is largely responsible for the reduction in the neointima-to-medial ratios seen in *Mkl1*$^{-/-}$ mice. Indeed, the numbers of Ki-67-positive proliferating cells within the injured vessels were also significantly lower in *Mkl1*$^{-/-}$ mice than in wild-type mice (Figure 2E and F). By contrast, the numbers of TUNEL-positive or cleaved caspase-3-positive apoptotic cells within the injured arteries did not differ between wild-type and *Mkl1*$^{-/-}$ mice (Supplementary Figure S2A through D). Similarly, the % fibrotic area in the media and intima and expression of the genes encoding collagen type 1 alpha1 and collagen type3 alpha1 within the injured arteries also did not significantly differ between wild-type and *Mkl1*$^{-/-}$ mice

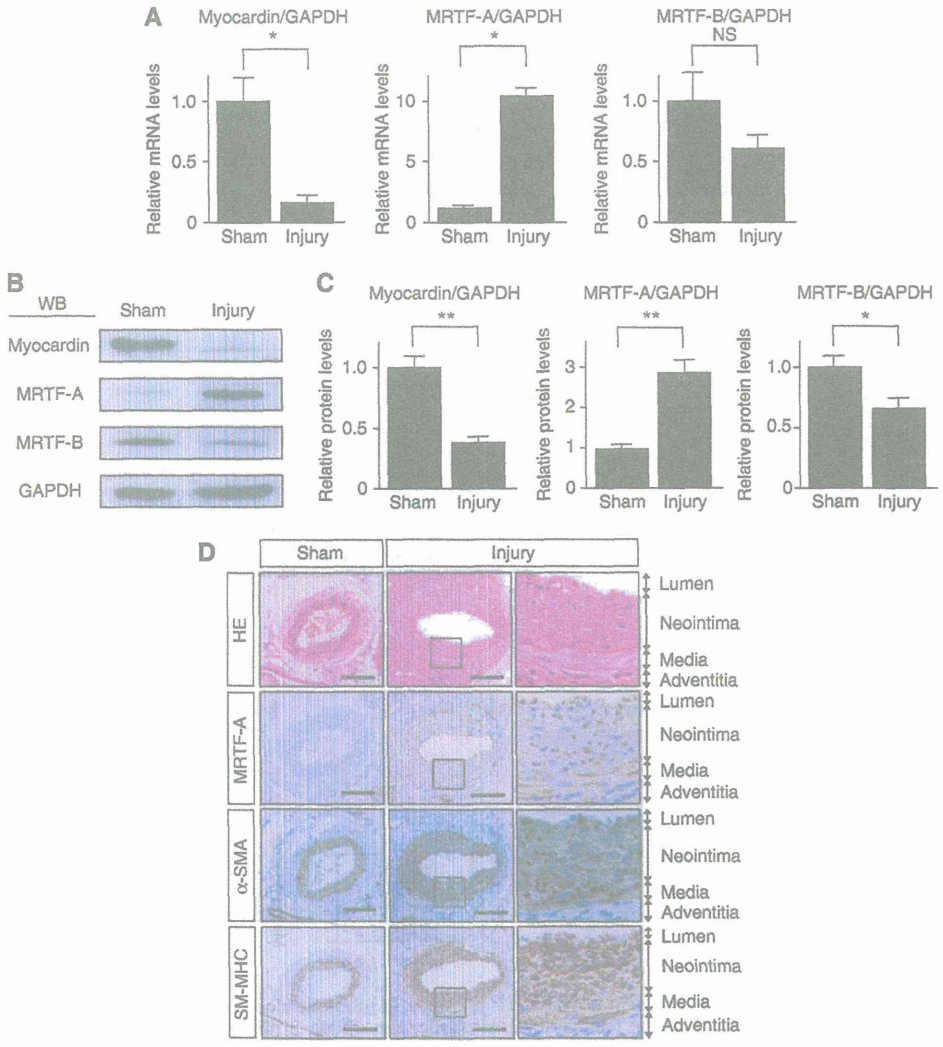

Figure 1 Increased expression of MRTF-A in femoral arteries after wire injury in mice. (**A**) Real-time RT–PCR analysis showing relative levels of myocardin, MRTF-A and MRTF-B mRNAs (normalized to GAPDH mRNA) in femoral arteries 2 weeks after wire injury (injury) ($n=6$ each). The relative mRNA level in sham-operated arteries (sham) was assigned a value of 1.0. (**B**) Representative western blots showing myocardin, MRTF-A and MRTF-B in wire-injured and sham-operated femoral arteries (2 weeks after injury). (**C**) The relative protein levels (normalized to GAPDH) of myocardin, MRTF-A and MRTF-B in wire-injured and sham-operated femoral arteries ($n=4$ each). The relative protein level in the sham-operated arteries was assigned a value of 1.0. (**D**) Immunohistochemical analysis of MRTF-A expression in sham-operated and wire-injured femoral arteries. Tissues are labelled with anti-BSAC (MRTF-A), anti-α-smooth muscle actin (αSMA) or anti-smooth muscle myosin heavy chain (SM-MHC) antibodies; bar indicates 100 μm. Three different experiments gave identical results. All graphs are shown as means ± s.e.m. $^{*}P<0.05$. $^{**}P<0.001$. NS, not significant. Figure source data can be found with the Supplementary data.

(Supplementary Figure S2E through G). In addition, because multiple cell types other than dedifferentiated VSMCs can contribute to neointima formation and to the vascular remodelling process, we also stained the tissue for endothelial cell (CD31) and macrophage (Mac3) markers. The relative numbers of CD31-positive and Mac3-positive cells in the injured arteries did not differ between wild-type and *Mkl1*$^{-/-}$ mice (Figure 2G through I), which indicates that a reduction in the number of αSMA-positive dedifferentiated VSMCs contributes to the attenuation of vascular remodelling in wire-injured *Mkl1*$^{-/-}$ mice. We also examined neointima formation following carotid artery ligation in *Mkl1*$^{-/-}$ mice, and found that neointima formation 4 weeks after carotid ligation was significantly diminished in *Mkl1*$^{-/-}$ mice, as compared to control *Mkl*$^{+/-}$ mice (Supplementary Figure S2H and I; Supplementary Table S1).

Loss of MRTF-A attenuates atherosclerotic lesions in APOE$^{-/-}$ *mice*

We next sought to analyse MRTF-A expression in a model of a different type of vascular disorder. *ApoE*$^{-/-}$ mice are prone to atherosclerotic lesions, to which both dedifferentiated VSMCs and infiltrating inflammatory cells contribute (Glass and Witztum, 2001; Bentzon *et al*, 2006). MRTF-A gene expression was significantly upregulated in aortic tissues containing atherosclerotic lesions in *ApoE*$^{-/-}$ mice fed a high cholesterol diet for 8 weeks (from 8 to 16 weeks of age), as compared to normal wild-type aortic tissues in

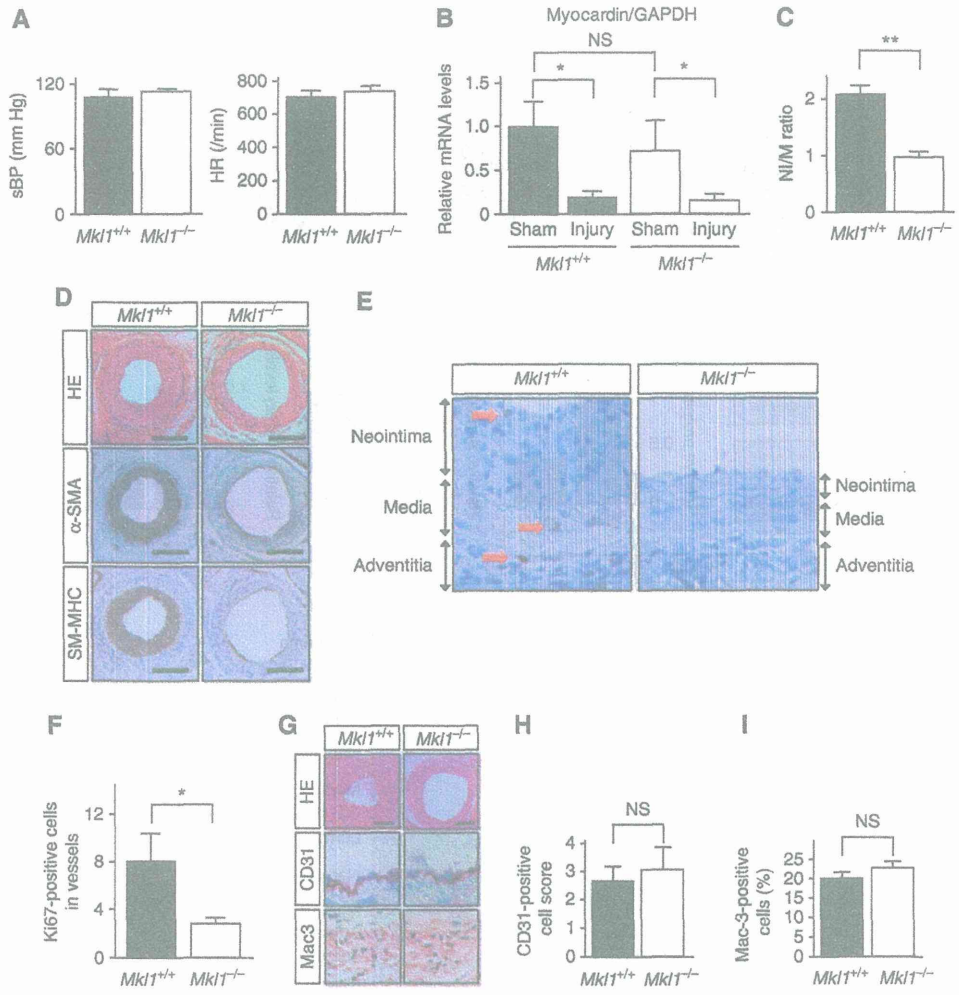

Figure 2 Attenuated vascular remodelling in response to wire injury in *Mkl1*$^{-/-}$ mice. (**A**) Systolic blood pressure (sBP) and heart rate (HR) in control *Mkl1*$^{+/+}$ and *Mkl1*$^{-/-}$ mice ($n=5$ each). (**B**) The relative levels of myocardin mRNA in wire-injured and sham-operated femoral arteries in *Mkl1*$^{+/+}$ and *Mkl1*$^{-/-}$ mice ($n=5$ each). (**C**) The neointima (NI)-to-media (M) ratio in arteries 4 weeks after wire injury in *Mkl1*$^{+/+}$ and *Mkl1*$^{-/-}$ mice ($n=20$ each). (**D**) Representative images of neointima in arteries 4 weeks after wire injury in *Mkl1*$^{+/+}$ and *Mkl1*$^{-/-}$ mice. HE: haematoxylin-eosin staining. α-SMA: staining with anti-α-SMA antibody. SM-MHC: staining with anti-SM-MHC antibody. (**E**) Representative images of neointima 4 weeks after femoral artery injury stained with anti-Ki-67 antigen in *Mkl1*$^{+/-}$ and *Mkl1*$^{-/-}$ mice. Red arrows indicate Ki-67-positive cells. (**F**) Numbers of Ki-67-positive cells in injured vessels of *Mkl1*$^{+/+}$ and *Mkl1*$^{-/-}$ mice 4 weeks after wire injury are shown ($n=3$ in each group). (**G**) Representative images of neointima stained with anti-CD31 (CD31) or anti-Mac3 (Mac3) antibody in arteries from *Mkl1*$^{+/+}$ and *Mkl1*$^{-/-}$ mice 4 weeks after wire injury. (**H, I**) The semi-quantitative CD31-positive scores ($n=5$ in each group) (**H**) and the relative numbers of Mac3-positive cells (% positive cells/total cells in neointima and media; $n=4$ in each group) (**I**) in *Mkl1*$^{+/+}$ and *Mkl1*$^{-/-}$ mice 4 weeks after wire injury are shown. All graphs are shown as means ± s.e.m. *$P<0.05$. **$P<0.001$. NS, not significant.

Table I Luminal and neointimal area of femoral arteries 4 weeks after vascular injury

	n	Lumen ($\times 10^3/\mu m^2$)	Intima ($\times 10^3/\mu m^2$)	Media ($\times 10^3/\mu m^2$)	IEL ($\times 10^3/\mu m^2$)	EEL ($\times 10^3/\mu m^2$)	Intima/Media ratio
Mkl1$^{+/+}$ sham	4	11.9 ± 2.7	0	19.0 ± 1.2	11.9 ± 2.7	30.9 ± 3.3	0
Mkl1$^{-/-}$ sham	4	10.4 ± 2.8	0	20.2 ± 2.5	10.4 ± 2.8	30.6 ± 2.8	0
Mkl1$^{+/+}$ injury	20	24.9 ± 3.5	39.7 ± 5.0	18.8 ± 1.1	64.8 ± 4.6	84.0 ± 5.4	2.09 ± 0.17
Mkl1$^{-/-}$ injury	20	29.6 ± 3.9	22.0 ± 2.3*	22.7 ± 1.2	52.3 ± 4.6	75.3 ± 5.3	0.96 ± 0.10*

The ratio of intima to media was calculated as the intimal area/medial area. Values are means ± s.e.m. IEL, internal elastic lamina; EEL, external elastic lamina. *$P<0.01$ versus *Mkl1*$^{+/+}$ injured arteries.

age-matched mice (Figure 3A). By contrast, myocardin gene expression was significantly decreased in atherosclerotic aortas, compared to normal aortas (Figure 3A). Consistent with that finding, cells positively stained for MRTF-A were observed within atherosclerotic lesions in the proximal aorta of *ApoE*$^{-/-}$ mice (Figure 3B).

To evaluate directly the contribution of MRTF-A to the development of atherosclerotic lesions in *ApoE*$^{-/-}$ mice, we crossed *Mkl1*$^{-/-}$ and *Apo E*$^{-/-}$ mice. Although the blood pressures, heart rates, cholesterol profiles and myocardin gene expression in aortic tissues did not differ between *Mkl1*$^{+/+}$;*ApoE*$^{-/-}$ and *Mkl1*$^{-/-}$;*ApoE*$^{-/-}$ mice

(Supplementary Figure S3A; Figure 3C), en-face analysis of the global progression of atherosclerotic lesions throughout the aorta revealed that the aortas of *Mkl1*$^{-/-}$;*ApoE*$^{-/-}$ mice contained smaller atherosclerotic lesions than those of *Mkl1*$^{+/+}$;*ApoE*$^{-/-}$ mice (Figure 3D). Furthermore, cross-sectional analysis of the proximal aorta revealed the average lesion area at the aortic root of *Mkl1*$^{-/-}$;*ApoE*$^{-/-}$ mice (2.5%) to be significantly smaller than at the aortic root of *Mkl1*$^{+/+}$; *ApoE*$^{-/-}$ mice (11.8%, $P<0.05$ versus *Mkl1*$^{-/-}$;*ApoE*$^{-/-}$) (Figure 3E and F). The relative accumulation of macrophages within atherosclerotic lesions at the aortic root, which was estimated based on the size of the

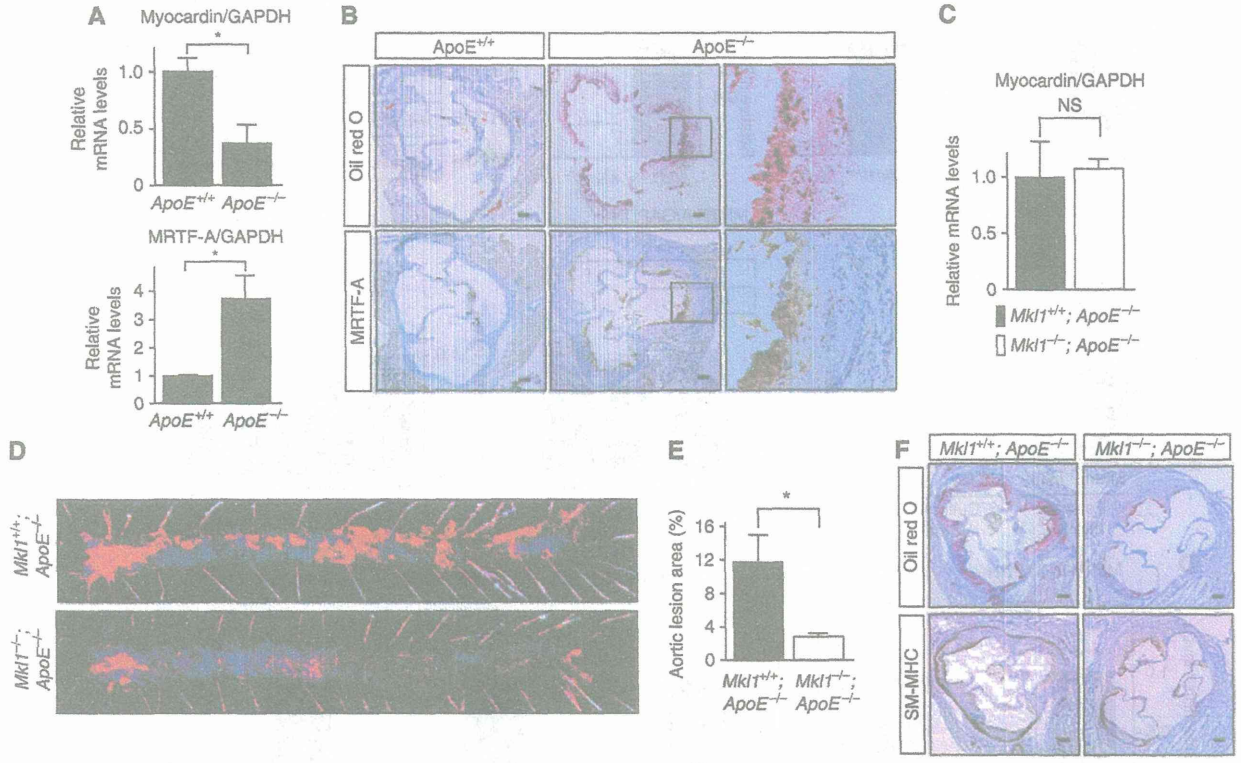

Figure 3 Atherosclerotic lesions in *Mkl1*$^{-/-}$;*ApoE*$^{-/-}$ mice are attenuated, as compared to those in *Mkl1*$^{+/+}$;*ApoE*$^{-/-}$ mice. (**A**) Real-time RT–PCR analysis showing the relative levels of MRTF-A and myocardin mRNAs (normalized to GAPDH mRNA) in atherosclerotic aortas from *ApoE*$^{-/-}$ mice fed a high-cholesterol diet and normal aortas from *ApoE*$^{+/+}$ mice at 16 weeks of age ($n=4$ each). *$P<0.05$. (**B**) Representative images showing MRTF-A expression within an atherosclerotic lesion in the proximal aorta of *ApoE*$^{-/-}$ mice. The tissues from *Apo*$^{+/+}$ and *ApoE*$^{-/-}$ mice were stained using anti-BSAC antibodies (MRTF-A). Oil-red O: Oil-red O staining. Three different experiments gave identical results. (**C**) Real-time RT–PCR analysis showing the relative levels of myocardin mRNA in atherosclerotic aortas from *Mkl1*$^{-/-}$;*ApoE*$^{-/-}$ and *Mkl1*$^{+/+}$;*ApoE*$^{-/-}$ mice fed a high-cholesterol diet ($n=4$ each). (**D**) Representative images of atherosclerotic lesions from an en-face analysis of the total aorta in *Mkl1*$^{+/+}$;*ApoE*$^{-/-}$ and *Mkl1*$^{-/-}$;*ApoE*$^{-/-}$ mice fed a high-cholesterol diet. Sudan III staining. Three independent experiments showed identical results. Red colour shows lipid-laden areas representing atherosclerotic lesions. (**E**) Graphs showing the relative (%) area of atherosclerotic lesions in cross-sections of proximal aorta from *Mkl1*$^{+/+}$;*ApoE*$^{-/-}$ and *Mkl1*$^{-/-}$;*ApoE*$^{-/-}$ mice fed a high-cholesterol diet for 8 weeks ($n=8$ each). *$P<0.05$. (**F**) Representative images of atherosclerotic lesions in cross-sections of proximal aorta from *Mkl1*$^{+/+}$;*ApoE*$^{-/-}$ and *Mkl1A*$^{-/-}$;*ApoE*$^{-/-}$ mice fed a high-cholesterol diet. Oil-red O: Oil-red O staining. SM-MHC: staining with anti-SM-MHC antibody. Bar indicates 100 μm. All graphs are shown as means ± s.e.m.

Figure 4 MRTF-A mediates acquisition of migration capacity by dedifferentiated VSMCs through regulation of SRF-target genes. (**A**) Real-time RT–PCR analysis showing relative levels of vinculin, MMP9 and integrin β1 mRNAs (normalized to GAPDH mRNA) in femoral arteries 2 weeks after wire injury in *Mkl1*$^{+/+}$ and *Mkl1*$^{-/-}$ mice ($n=4$ each). (**B**) Representative western blots showing myocardin, MRTF-A and MRTF-B in arteries 2 weeks after wire injury, in sham-operated arteries and in cultured mouse aortic VSMCs (MAVSMCs) and rat aortic VSMCs (RAVSMCs). (**C**) Real-time RT–PCR analysis showing the relative levels of myocardin, MRTF-A and MRTF-B mRNAs in femoral arteries 2 weeks after wire injury (injury), in sham-operated arteries (sham) and in cultured MAVSMCs and RAVSMCs ($n=6$ each). (**D**) Real-time RT–PCR analysis showing relative levels of MRTF-A, myocardin, vinculin, MMP9 and integrin β1 mRNAs in RAVSMCs transfected with MRTF-A siRNA or control siRNA ($n=6$ each). (**E**) Co-transfection of a plasmid expressing MRTF-A (0, 10 and 100 ng) plus the luciferase reporter gene driven by bp −360 to +63 of the 5′-flanking region of vinculin gene (vinculin-luc) into RAVSMCs (left panel) and NIH3T3 cells (right panel). Relative luciferase activities normalized to Renilla luciferase (pRL-TK) activity are shown. Vinculin CArG-mut-luc: luciferase reporter gene driven by the vinculin promoter harbouring a mutation within the CArG-box. Data were obtained from three experiments performed in sextuplicate. (**F**) Co-transfection of MRTF-A siRNA plus vinculin-luc into RAVSMCs. Relative luciferase activities normalized to Renilla luciferase activity are shown. Data were obtained from two experiments performed in sextuplicate. (**G**) Migration in the presence or absence of PDGF-BB of RAVSMCs transfected with MRTF-A siRNA or control siRNA. Data were obtained from three experiments performed in sextuplicate. (**H**) Proliferation in the presence or absence of fetal calf serum (FCS) of RAVSMCs transfected with MRTF-A siRNA or control siRNA. Data were obtained from three experiments performed in sextuplicate. All graphs are shown as means ± s.e.m. *$P<0.05$ and **$P<0.01$. NS, not significant. Figure source data can be found with the Supplementary data.

F4/80-stained area normalized to the corresponding total atherosclerotic lesion area, did not significantly differ between *Mkl1*$^{+/+}$;*ApoE*$^{-/-}$ and *Mkl1*$^{-/-}$;*ApoE*$^{-/-}$ mice (Supplementary Figure S3B).

MRTF-A is necessary for acquisition of migratory capacity in dedifferentiated VSMCs

SRF controls cellular migration capacity in various cell types, including dedifferentiated VSMCs, by regulating the expres-

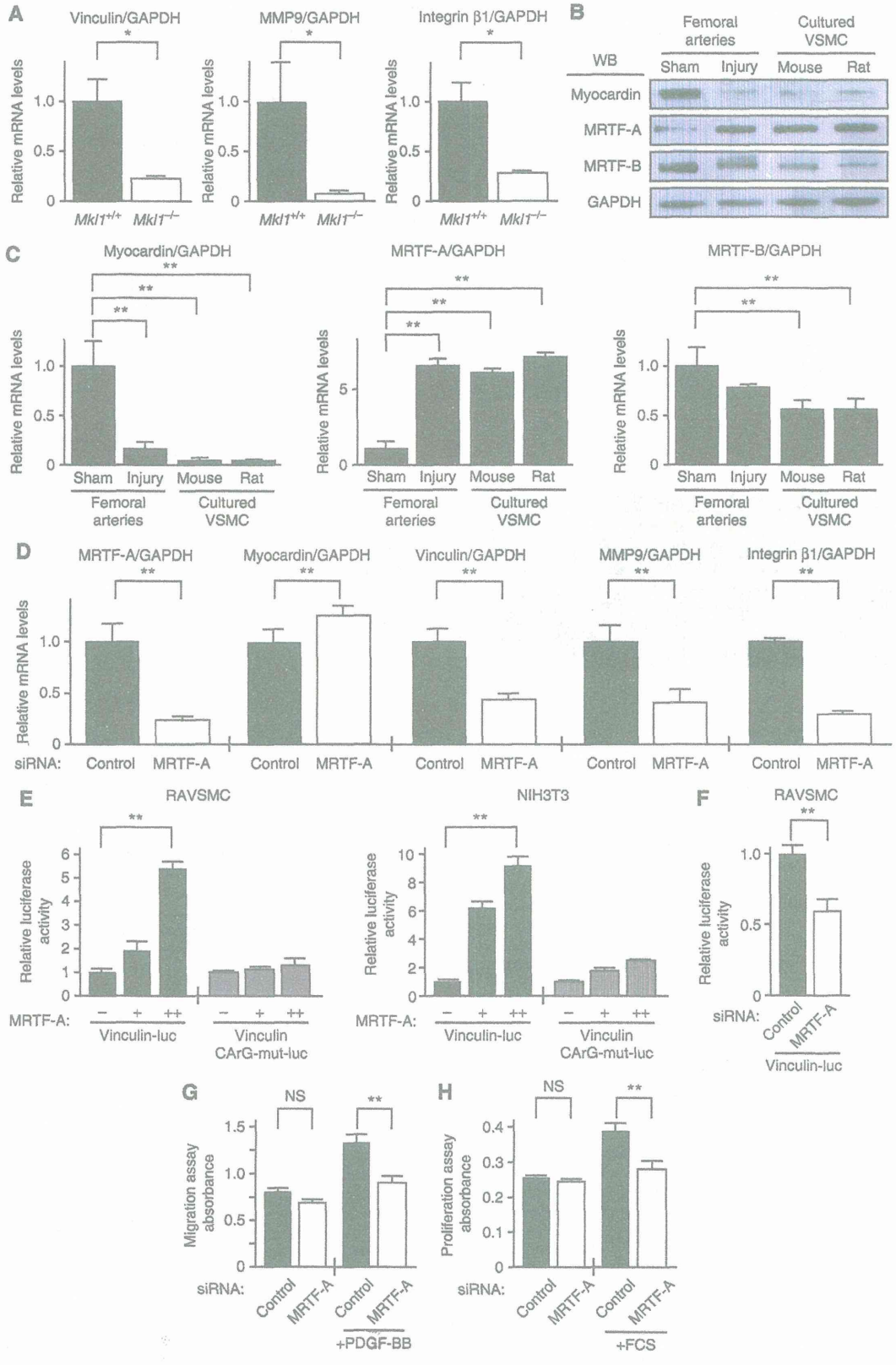

sion of several target genes, including the genes encoding vinculin, MMP9 and integrin β1 (Kenagy *et al*, 1997; Xu *et al*, 1998; Morita *et al*, 2007; Medjkane *et al*, 2009; Olson and Nordheim, 2010). We therefore examined the expression of these SRF-target genes in wire-injured femoral arteries. We found that 2 weeks after wire injury there was significantly less expression of vinculin, MMP9 and integrin β1 genes in the injured femoral arteries of *Mkl1*$^{-/-}$ mice than control *Mkl1*$^{+/+}$ mice (Figure 4A). The expression of these genes in the intact femoral arteries of *Mkl1*$^{-/-}$ and control *Mkl1*$^{+/+}$ mice was not significantly different (Supplementary Figure S4A). The mRNA expression of other SRF targets, αSMA (*ACTA2*) and SM-MHC (*Myh11*) genes encoding smooth muscle-specific contractile proteins, was also significantly less in the injured femoral arteries of *Mkl1*$^{-/-}$ mice than *Mkl1*$^{+/+}$ mice (Supplementary Figure S4B). In primary mouse aortic VSMCs (MAVSMCs), a cellular model of dedifferentiated VSMCs in which MRTF-A expression is increased and myocardin expression is decreased (Figure 4B and C; Supplementary Figure S4C; Hinson *et al*, 2007; Nakamura *et al*, 2010), levels of vinculin, MMP9, integrin β1 and αSMA mRNA were significantly reduced after knocking down MRTF-A (Figure 4D; Supplementary Figure S4D). This suggests that MRTF-A plays a predominant role in maintaining the expression of several SRF-target genes involved in cellular migration in dedifferentiated VSMCs, where expression of myocardin is decreased (Figure 4B and C; Nakamura *et al*, 2010). Overexpression of MRTF-A stimulated vinculin promoter activity in an SRF-dependent manner in both primary rat aortic VSMCs (RAVSMCs) and NIH3T3 fibroblasts (Figure 4E), whereas knocking down MRTF-A reduced vinculin promoter activity in RAVSMCs (Figure 4F). This supports the conclusion that MRTF-A regulates the expression of SRF-target genes in dedifferentiated VSMCs. Furthermore, knocking down MRTF-A significantly impaired PDGF-BB-induced RAVSMC migration, whereas knocking down myocardin did not (Figure 4G; Supplementary Figure S4E and F).

Because SRF is also known to control cellular proliferation, we examined the effect of MRTF-A knockdown on RAVSMC proliferation, and found that knocking down MRTF-A significantly reduced serum-induced RAVSMC proliferation, whereas knocking down myocardin did not (Figure 4H; Supplementary Figure S4G).

Reduced miR-1 expression contributes to the increase in MRTF-A expression in dedifferentiated VSMCs

We next investigated the molecular mechanisms potentially involved in regulating the reciprocal expression of MRTF-A and myocardin during VSMC dedifferentiation. We initially hypothesized that increased expression of myocardin leads to the repression of MRTF-A gene transcription through either direct or indirect mechanisms. Within the MRTF-A gene, the 5′-flanking region (FR) up to 1 kbp from the transcription start site is well conserved among different species. However, we failed to detect any significant effects of myocardin or MRTF-A on the activity of −930 bp MRTF-A promoter region in either RAVSMCs or NIH3T3 cells (Figure 5A; Supplementary Figure S5A). Myocardin also did not significantly affect the promoter activity of −5500 bp MRTF-A promoter region in either RAVSMCs or NIH3T3 cells (Supplementary Figure S5B). We therefore focused on the role of the 3′-untranslated region (UTR) of MRTF-A mRNA, where we found a conserved target site for microRNA-1 (miR-1) (Figure 5B). We observed that expression of miR-1 in vascular tissues is >100 times higher than in several non-muscle tissues, though its expression in skeletal and cardiac muscle tissues is much higher (Figure 5C). Consistent with earlier reports that miR-1 expression is regulated by myocardin and SRF in VSMCs and is downregulated in neointimal lesions created by ligation of carotid arteries of mice (Zhao *et al*, 2005; Chen *et al*, 2011), miR-1 expression was significantly weaker in the injured femoral arteries and atherosclerotic aorta of *ApoE*$^{-/-}$ mice, where there was a corresponding reduction of myocardin expression, than in control arteries (Figures 1A through C and 5D; Supplementary Figure S5C). Levels of miR-1 expression were also substantially lower in cultured RAVSMCs than in normal arteries (Supplementary Figure S5D). Overexpression of a miR-1 mimic significantly reduced endogenous MRTF-A gene and protein expression in RAVSMCs (Figure 5E and F), whereas overexpression of a miR-1 inhibitor significantly increased MRTF-A mRNA and protein expression (Figure 5G and H).

We also assessed miR-1-induced repression of MRTF-A gene by placing its 3′-UTR downstream of a cytomegalovirus (CMV)-driven luciferase reporter and performing luciferase assays in COS7 cells transfected with a miR-1 mimic or control scrambled oligo (Figure 5I). The miR-1 mimic significantly reduced the activity of the luciferase reporter linked to the MRTF-A 3′-UTR, and a mutation in the predicted miR-1 binding site in the 3′-UTR prevented that repression (Figure 5J). Moreover, overexpression of myocardin in A7r5 VSMCs significantly repressed the activity of a luciferase reporter gene linked to the MRTF-A 3′-UTR in a miR-1-dependent fashion (Figure 5K). These results strongly suggest that reduced expression of miR-1 caused by the reduction in myocardin expression during the process of phenotypic modulation of VSMCs contributes to the increase in MRTF-A expression in dedifferentiated VSMCs. Consistent with those findings, injection of an anti-miR-1 Locked Nucleic Acid (LNA)™-enhanced microRNA inhibitor into the injured vessels led to an increase in MRTF-A gene expression and exacerbated the pathological vascular remodelling after wire injury (Supplementary Figure S5E through G; Supplementary Table S2).

Pharmacological inhibition of MRTF-A activity attenuates adverse vascular remodelling after wire injury

The results presented raise the possibility that MRTF-A is a novel therapeutic target for the treatment of vascular disease. Recently, a small molecule (CCG-1423) was found to inhibit Rho pathway-mediated SRF activation (Evelyn *et al*, 2007; Jin *et al*, 2011). CCG-1423 appears to inhibit the interaction between SRF and MRTF-A at a point upstream of the DNA binding. Although the site of inhibition and its selectivity is not yet precisely defined, it was recently shown that CCG-1423 blocks nuclear translocation of MRTF-A, thereby inhibiting MRTF-A-mediated effects on SRF transcription, at least in part (Jin *et al*, 2011). In addition, we confirmed that CCG-1423 blocks serum-induced nuclear accumulation of endogenous MRTF-A in RAVSMCs (Figure 6A). CCG-1423 also significantly blocked SRF activity induced by co-expres-

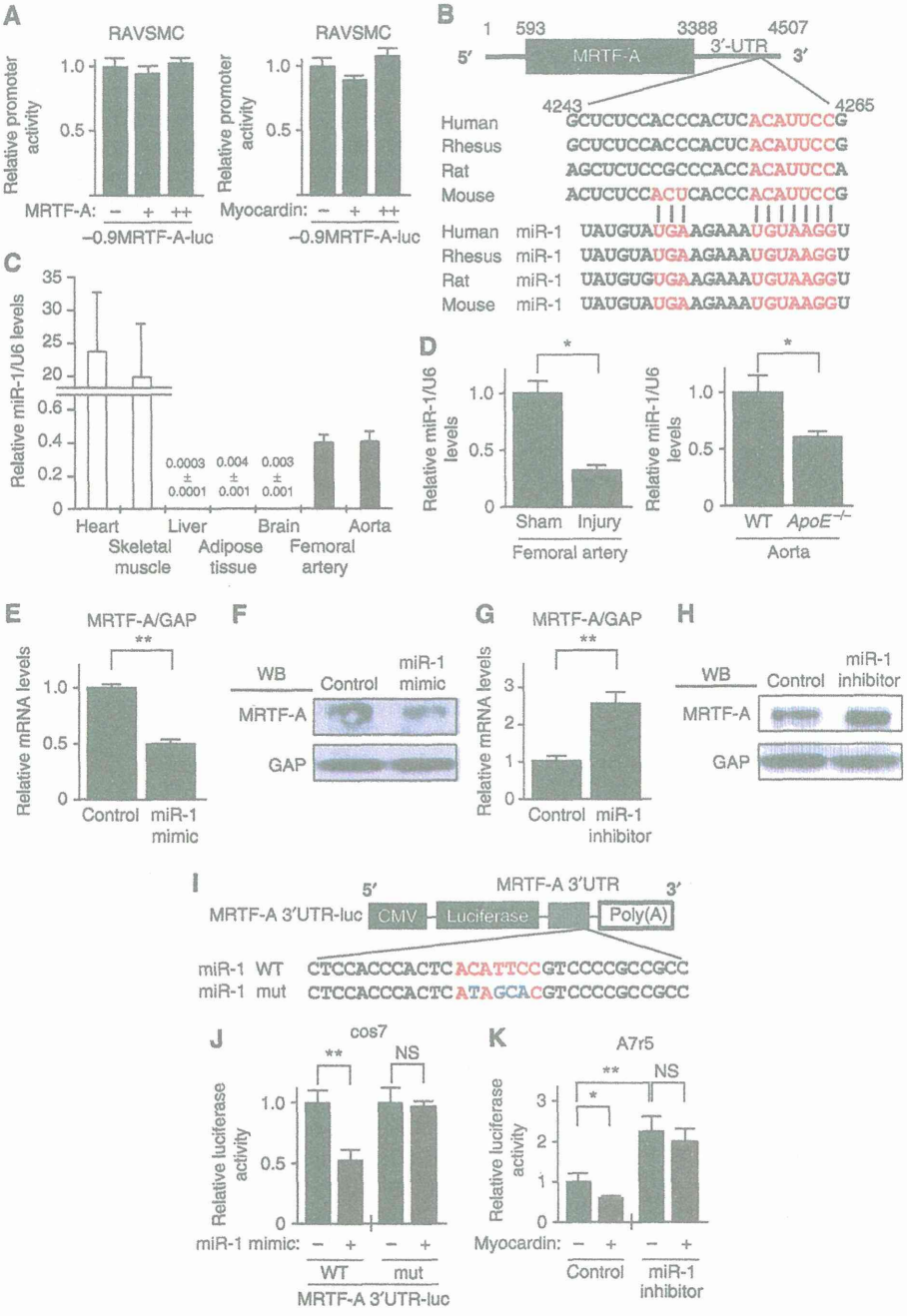

Figure 5 MicroRNA-1 regulates MRTF-A gene expression. (**A**) Co-transfection of a plasmid encoding myocardin or MRTF-A (0, 10 and 100 ng) with the −930 bp MRTF-A-luc gene into RAVSMCs. Data were obtained from two experiments performed in quadruplicate. +: 10 ng. ++: 100 ng. (**B**) Schematic representation of the MRTF-A 3′-untranslated region (UTR) containing a conserved microRNA-1 (miR-1) target site (shown in red). Sequences of mature miR-1 in different species are shown below. (**C**) Real-time RT–PCR analysis showing the relative miR-1 expression (normalized to the U6 levels) in different mouse tissues. (**D**) Real-time RT–PCR analysis showing the relative miR-1 expression (normalized to the U6 levels) in femoral arteries 2 weeks after wire injury or sham operation in wild-type mice ($n=4$ each) (left panel), and in aortic tissues in *ApoE*$^{-/-}$ or control wild-type mice (right panel). (**E**) Endogenous expression of MRTF-A mRNA in RAVSMCs transfected with miR-1 mimic or control oligo. Graphs show the relative MRTF-A mRNA levels (normalized to GAPDH mRNA) ($n=4$ each). (**F**) Representative western blots showing the effect of miR-1 mimic on MRTF-A expression in RAVSMCs. Three different experiments gave identical results. (**G**) Endogenous MRTF-A mRNA expression in RAVSMCs transfected with miR-1 inhibitor. Graphs show the relative MRTF-A mRNA levels ($n=4$ each). (**H**) Representative western blots showing the effect of a miR-1 inhibitor on MRTF-A expression in RAVSMCs. Three different experiments gave identical results. (**I**) Luciferase reporter constructs containing wild-type and mutant MRTF-A 3′UTR (MRTF-A 3′UTR-luc and mutMRTF-A 3′UTR-luc, respectively). The conserved miR-1 target site is shown in red. In mutMRTF-A 3′UTR-luc, mutations were introduced within the miR-1 target site (shown in blue). (**J**) MRTF-A 3′UTR-luc and mutMRTF-A 3′UTR-luc were co-transfected with miR-1 mimic into COS7 cells for 48 h. Data were obtained from three experiments performed in quadruplicate. (**K**) MRTF-A 3′UTR-luc was transfected with or without a plasmid expressing myocardin and/or a miR-1 inhibitor into A7r5 cells for 48 h. Data were obtained from three experiments performed in quadruplicate. All graphs are shown as means ± s.e.m. Relative luciferase activities normalized to control Renilla luciferase activity are shown. *$P<0.05$. **$P<0.01$. NS, not significant. Figure source data can be found with the Supplementary data.

sion of striated muscle activator of rho signalling (STARS) and MRTF-A in RAVSMCs (Figure 6B; Kuwahara *et al*, 2005). STARS is an actin-binding protein that activates SRF by inducing nuclear accumulation of MRTF-A. Both CCG-1423 and MRTF-A knockdown similarly inhibited STARS-induced activation of SRF in RAVSMCs. Furthermore, this inhibitory effect of CCG-1423 on STARS-induced activation of SRF was abolished by knocking down MRTF-A, supporting the notion that CCG-1423 blocks MRTF-A-mediated activation of SRF (Supplementary Figure S6A) Similarly to knocking down MRTF-A, CCG-1423 significantly reduced the migration and proliferation capacities of RAVSMCs (Figure 6C and D). When we then treated mice subjected to femoral artery wire injury with CCG-1423 (0.15 mg/kg intraperitoneally for 3 weeks), we found that CCG-1423 significantly attenuated the progression of vascular remodelling in arteries 3 weeks after injury (Figure 6E and F; Table II; Supplementary Figure S6B and C), without affecting the hemodynamic parameters or cholesterol profiles (Supplementary Figure S6D and E). CCG-1423 did not affect gross appearance, body weight or survival among the mice during the experiment (data not shown). Furthermore, administration of CCG-1423 also significantly attenuated the

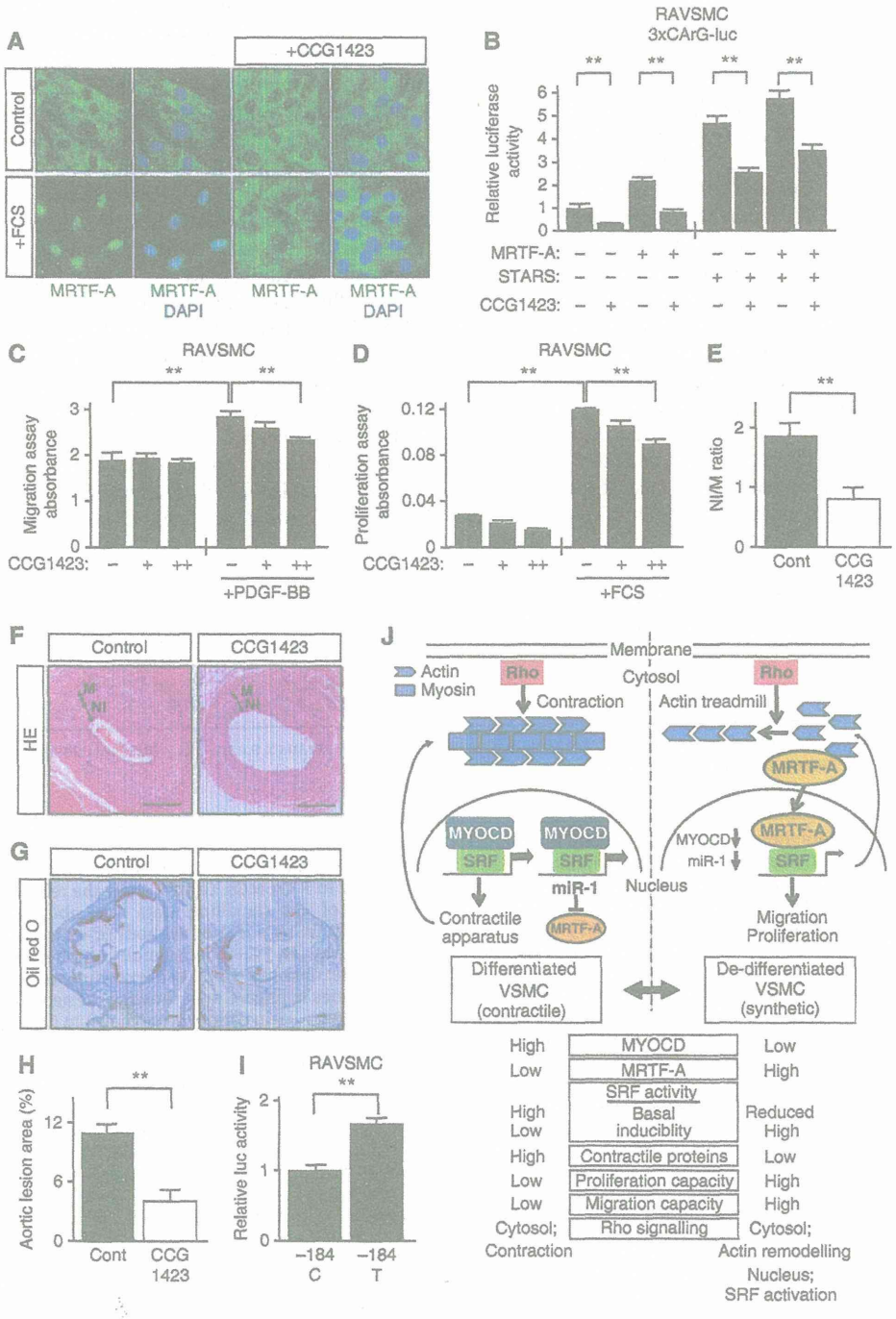

development of atherosclerotic lesions in *ApoE*$^{-/-}$ mice fed a high cholesterol diet for 6 weeks (Figure 6G and H; Supplementary Figure S6F).

Recently, it has been revealed that an SNP in the promoter region of the human MRTF-A gene (−184C>T), which results in a high transcriptional activity in HeLa and K562 cells, is associated with susceptibility to CAD (Hinohara *et al*, 2009). We found that the −930 bp of MRTF-A promoter containing −184T, which is associated with high CAD susceptibility, showed significantly stronger transcriptional activity than the wild-type promoter in cultured RAVSMCs (Figure 6I). These results further support our notion that inhibition of MRTF-A could be an effective novel approach to the treatment and prevention of vascular disorders.

Discussion

In the present study, we used three vascular injury models (femoral artery wire injury, carotid artery ligation and diet-induced atherosclerosis in *APOE*$^{-/-}$ mice) in *Mkl1*$^{-/-}$ mice to elucidate the roles played by MRTF-A in pathological vascular remodelling. We initially found that expression of MRTF-A mRNA and protein was significantly increased in injured arteries and aortic tissues containing atherosclerotic lesions in *ApoE*$^{-/-}$ mice, while expression of myocardin was reciprocally decreased. In each model, neointima formation or atherosclerotic lesions were significantly smaller in *Mkl1*$^{-/-}$ mice than in the respective controls. The expression of vinculin, MMP-9 and integrin β1 genes, which are targets of SRF and key regulators of cellular migration, was significantly diminished in the injured arteries of *Mkl1*$^{-/-}$ mice. Knocking down MRTF-A in RAVSMCs reduced expression of these genes in response to extracellular stimuli, which significantly impaired cell migration. These results demonstrate that induced expression of MRTF-A is crucial for acquisition of the capacity to migrate in response to environmental stress in dedifferentiated VSMCs (Liu *et al*, 2005). We also found that MRTF-A gene expression in VSMCs is, at least in part, regulated by miR-1, which is in turn regulated by myocardin and SRF (Jiang *et al*, 2010; Chen *et al*, 2011). Expression of miR-1 was reduced in dedifferentiated VSMCs, along with that of myocardin. This apparently led to an increase in MRTF-A expression, though it is possible that another as yet unidentified mechanism, such as transcriptional regulation through sites located in the distal 5′-FR or within introns, also contribute to the reciprocal regulation of myocardin and MRTF-A expression. Finally, we showed that a small molecule inhibitor of MRTF-A, CCG-1423, significantly reduced neointima formation following wire injury to mouse femoral arteries. Collectively, these results demonstrate that induction of MRTF-A plays a key role in vascular remodelling by maintaining SRF activity, thereby conferring a capacity for migration in response to extracellular stimuli on dedifferentiated VSMCs. MRTF-A is thus a potentially useful therapeutic target that may be more specific and efficient than the upstream Rho family GTPases, which can affect diverse intracellular signalling events.

In differentiated VSMCs, myocardin strongly activates SRF and the expression of VSMC-specific contractile proteins, thereby contributing to the maintenance of the contractile phenotype (Wang *et al*, 2003). Myocardin is constitutively located in the nucleus, where it suppresses MRTF-A expression via activation of miR-1. The ability of MRTF-B to transduce Rho signalling into the nucleus is much weaker than that of MRTF-A (Kuwahara *et al*, 2005; Nakamura *et al*, 2010),

Table II Luminal and neointimal area of femoral arteries 3weeks after vascular injury

	n	Lumen ($\times 10^3/\mu m^2$)	Intima ($\times 10^3/\mu m^2$)	Media ($\times 10^3/\mu m^2$)	IEL ($\times 10^3/\mu m^2$)	EEL ($\times 10^3/\mu m^2$)	Intima/Media ratio
Control injury	6	15.0±3.0	39.9±4.1	22.9±2.1	55.0±2.4	77.8±3.7	1.85±0.17
CCG1423 injury	8	22.3±5.6	20.2±4.8*	24.8±1.6	43.0±7.2	67.8±2.8	0.81±0.19*

The ratio of intima to media was calculated as the intimal area/medial area. Values are means±s.e.m. IEL, internal elastic lamina; EEL, external elastic lamina. *$P<0.01$ versus control injured arteries.

Figure 6 CCG-1423, an MRTF-A inhibitor, attenuated neointima formation induced by wire injury in mouse femoral arteries. (**A**) CCG-1423 diminished the nuclear accumulation of endogenous MRTF-A induced by 20% FCS in RAVSMCs. Cells were stained with anti-MRTF-A antibody (green) and DAPI (blue). (**B**) CCG-1423 significantly inhibited MRTF-A-induced SRF activity in RAVSMCs. Graphs show the relative luciferase activities of 3 × CArG-luc. STARS: expression plasmid encoding striated muscle activator of Rho signalling. Data were obtained from two experiments performed in quintuplicate. (**C**) PDGF-BB-induced migration was assessed in RAVSMCs treated without or with 0.1 μm (+) or 1 μm (++) of CCG-1423. Data were obtained from two experiments performed in sextuplicate. (**D**) FCS-induced proliferation was assessed in RAVSMCs treated without or with 0.1 μm (+) or 1 μm (++) of CCG-1423. Data were obtained from two experiments performed in quadruplicate. (**E, F**) Effect of CCG-1423 on neointima formation in wire-injured femoral arteries in mice. Graph showing the neointima (NI)-to-media (M) ratio in wire-injured arteries from mice treated without (control) or with CCG-1423 ($n=3$ in control group and 4 in CCG1423 group) (**E**). Representative images of neointima are shown (**F**). (**G**) Representative images of atherosclerotic lesions in cross-sections of proximal aorta from *ApoE*$^{-/-}$ mice fed a high-cholesterol diet with or without CCG-1423 for 6 weeks. Oil-red O: Oil-red O staining. Bar indicates 100 μm. (**H**) Graphs showing the relative (%) area of atherosclerotic lesions in cross-sections of proximal aorta from *ApoE*$^{-/-}$ mice fed a high-cholesterol diet and treated with or without CCG-1423 for 6 weeks ($n=3$ in control group and 4 in CCG-1423 group). **$P<0.01$. (**I**) Effect of an SNP in the promoter region of MRTF-A gene (−184C>T) on the promoter activity in RAVSMCs. Relative activities of −930 bp MRTF-A(−184C)-luc and −930 bp MRTF-A(−184T)-luc in two different experiments performed in quadruplicate are shown. All graphs are shown as means±s.e.m. **$P<0.01$. (**J**) A proposed model of the role of MRTF-A in vascular remodelling. In differentiated, contractile VSMCs, constitutively nuclear myocardin strongly activates SRF, leading to expression of VSMC-specific contractile proteins, and suppresses MRTF-A expression through activation of miR-1. Under these conditions, cytosolic Rho signalling is confined almost exclusively to regulation of contraction. In dedifferentiated VSMCs, MRTF-A expression is induced by reductions in miR-1 expression and basal SRF activity, thereby maintaining the lower basal SRF activity necessary for cellular migration and proliferation. Because MRTF-A is shuttled between the cytosol and nucleus and because it activates SRF downstream of Rho signalling, in dedifferentiated VSMCs, extracellular stimuli activating Rho signalling can substantively affect cellular proliferation and migration by modulating SRF activity. MYOCD: myocardin.